Heavy-ion fusion using a parabolic barrier with Coulomb interaction

Q. Haider and F. Bary Malik
Department of Physics and Astronomy, Southern Illinois University-Carbondale, Carbondale, Illinois 62901
(Received 8 September 1981)

In this work, we describe the fusion mechanism between two heavy ions as penetration through a parabolic barrier in the presence of a proper Coulomb interaction with appropriate boundary conditions. The parabolic potential is matched to the Coulomb potential in order to avoid any discontinuity of the potential surface. The Schrödinger equations in the exterior and interior regions containing, respectively, the Coulomb and the parabolic potentials, are solved and the penetrability function is calculated from the logarithmic derivative at the matching radius. The theory is then applied to calculate the fusion cross sections for the reactions $^{16}O+^{16}O$, $^{12}C+^{28,29,30}Si$, $^{16}O+^{24,26}Mg$, $^{16}O+^{28,29,30}Si$, and $^{40}Ca+^{40}Ca$ and are found to reproduce the data quite well. The theory is valid for energies both below and above the barrier.

[NUCLEAR REACTIONS Heavy-ion fusion; effect of Coulomb interaction; analytic expression for the penetrability function; application to various reactions.]

I. INTRODUCTION

During the last few years, a wealth of data has been accumulated on fusion between heavy ions. In most of the reactions, the fusion cross section as a function of energy is found to exhibit small bumps or structures superimposed on a smooth background which reaches a maximum and then falls off slowly or saturates at higher energies. Several theoretical models[1] have been proposed to explain the data. Basically, two theoretical approaches have been made to explain the fusion mechanism and interpret the observed data. One approach attempts to understand these data using a complex optical potential with a repulsive core[2,3] and seems to do well near or below the Coulomb barrier. The other approach, which seems to be more successful at energies higher than the Coulomb barrier, attempts to describe the fusion process as penetration through a barrier often taken to be of a parabolic type.[4–7]

In the parabolic barrier approach, until recently, the penetrability function, $T_l(E)$, was calculated using the Hill-Wheeler expression[8]

$$T_l(E)=\{1+\exp[(2\pi/\hbar\omega)(V_{Bl}-E)]\}^{-1}, \quad (1)$$

where

$$V_{Bl}=V_B+\hbar^2 l(l+1)/(2\mu R_B{}^2), \quad (2)$$

and V_B and R_B are, respectively, the magnitude and location of the top of the s-wave barrier. μ, ω, and l are, respectively, the reduced mass, the oscillator frequency, and the orbital angular momentum. Both the approaches mentioned above relate the fusion cross section to the reaction cross section. However, as noted in Refs. 6 and 9–11, the Hill-Wheeler expression is inadequate to explain the fusion process at all energies especially in the presence of Coulomb interaction. Although Avishai's[10] and later Dethier and Stancu's[11] attempts to incorporate the Coulomb interaction have been partially successful at sub-Coulomb energies, their calculations cannot be used at energies near or above the barrier. Besides, in their treatment, the potential has a discontinuity near the top of the barrier for all partial waves. As shown by Dethier and Stancu,[11] this discontinuity results in an overestimation of the penetrability function for higher partial waves at energies well below the barrier top. Consequently, the effect of this discontinuity will be more pronounced for heavier nuclei where a larger number of partial waves contribute to the fusion process.

The purpose of this paper is to derive a proper expression for the penetrability function in the pres-

ence of Coulomb interaction which is valid for all orbital angular momenta and for all energies and is devoid of any discontinuity of the potential surface. In addition, we also incorporate the correct asymptotic form of the wave functions. The model is then used to calculate the fusion cross section for a number of reactions as well as determine the location and magnitude of the interaction barrier which the ions must overcome in order to reach the critical distance for fusion.

The paper is organized as follows. In Sec. II, we describe the model and the theoretical procedure used to calculate the penetrability function and hence the fusion cross section. Section III contains the numerical details. Results and discussion of our calculations are given in Sec. IV. In Sec. V, we conclude the paper.

II. THEORY

A. The model

While the parabolic potential is a good approximation to the real barrier in the region around the maximum that determines the essential features of the interaction, it completely ignores the long range effect of the Coulomb interaction. As such, its applicability may not be meaningful, particularly for particles with incident energies below the Coulomb barrier where the tail of the Coulomb potential goes to zero much more slowly than the parabolic barrier. Our aim, therefore, is to incorporate the effect of the Coulomb interaction into the fusion mechanism explicitly and then derive an analytic expression for the penetrability function which would be valid at all energies. In doing so, we retain the parabolic approximation only up to a certain distance R_n, which is taken to be the distance between the two ions when they just touch each other or are about to touch each other. R_n, however, should not be interpreted as the radius of fusion. For most systems, particularly the lighter ones, the fusion barrier occurs at very large distances outside the touching radius. This is discussed later in Sec. IV. Beyond R_n, the interaction is taken to be of a purely Coulomb type. We further impose the condition that the potential should be continuous and hence the Coulomb potential should match onto the parabolic one at $r=R_n$. This will eliminate the discontinuity in the potential which is present in the model of Avishai[10] and Dethier-Stancu.[11]

Thus we wish to consider penetration through a barrier given by

$$V_l(r)=\begin{cases} V_l-\frac{1}{2}\mu\omega^2(r-R_0)^2, & \text{for } r<R_n, \quad (3a)\\ Z_1Z_2e^2/r+\hbar^2 l(l+1)/(2\mu r^2), & \text{for } r>R_n, \quad (3b)\end{cases}$$

with the condition that the potentials match at $r=R_n$. Here, Z_1e and Z_2e are the Coulomb charges of the two ions. The matching condition at $r=R_n$ yields

$$V_l=V_0+\hbar^2 l(l+1)/(2\mu R_n^2)\ , \quad (4)$$

where

$$V_0=\tfrac{1}{2}\mu\omega^2(R_n-R_0)^2+Z_1Z_2e^2/R_n\ . \quad (5)$$

From this, the location of the barrier top is obtained at

$$R_0=R_n-[2(V_0-Z_1Z_2e^2/R_n)/(\mu\omega^2)]^{1/2}\ . \quad (6)$$

Our purpose here is to obtain the penetrability function, $T_l(E)$, through such a barrier. Once that is obtained, the fusion cross section, σ_f, is given by

$$\sigma_f=\pi\lambda\!\!\!^{-2}\sum_{l=0}^{\infty}(2l+1)T_l(E) \quad (7)$$

with

$$\lambda\!\!\!^{-1}=k=(2\mu E/\hbar^2)^{1/2}\ . \quad (8)$$

Here E is the center of mass energy.

$T_l(E)$ can be calculated by solving the Schrödinger equation in the exterior region having the potential (3b) and in the interior region having the potential (3a) and matching the two logarithmic derivatives using the boundary condition appropriate for transmission. Following Blatt and Weisskopf,[12] we note that the boundary condition for transmission requires that the logarithmic derivative of the wave function should be complex with the imaginary part less than zero.

B. Solution in the region $r>R_n$

We shall follow the procedure of Feshbach *et al.*,[13] which has been outlined in detail by Blatt and Weisskopf,[12] in developing the formulae in this section. In this region, there is only the Coulomb potential (3b) and the equation for $u_l(\rho)$ (r times the radial wave function) is

$$\frac{d^2u_l(\rho)}{d\rho^2}+\left[1-\frac{2\eta}{\rho}-\frac{l(l+1)}{\rho^2}\right]u_l(\rho)=0\ , \quad (9)$$

with $\rho=kr$ and

$$\eta=\mu Z_1Z_2e^2/(\hbar^2 k)\ .$$

The solution, $u_l(\rho)$, of the above differential equation can always be written in the form

$$u_l(\rho)=\mathrm{A}u_l^{(-)}(\rho)+\mathrm{B}u_l^{(+)}(\rho)\ , \tag{10}$$

where

$$u_l^{(+)}(\rho)=\exp(-i\sigma_l)[G_l(\rho)+iF_l(\rho)]\ , \tag{11}$$

$$u_l^{(-)}(\rho)=\text{complex conjugate of } u_l^{(+)}(\rho)\ , \tag{12}$$

are the outgoing and incoming waves, respectively. σ_l is the Coulomb phase shift; $F_l(\rho)$ and $G_l(\rho)$ are the "regular" and "irregular" Coulomb functions having the asymptotic forms

$$F_l(\rho)\underset{\rho\to\infty}{\sim}\sin(\rho-\pi l/2-\eta\ln 2\rho+\sigma_l)\ , \tag{13}$$

$$G_l(\rho)\underset{\rho\to\infty}{\sim}\cos(\rho-\pi l/2-\eta\ln 2\rho+\sigma_l)\ . \tag{14}$$

The logarithmic derivative at $r=R_n$, defined by

$$f_l=R_n\left[\frac{du_l/dr}{u_l}\right]_{r=R_n}\ , \tag{15}$$

finally gives for the penetrability function

$$T_l(E)=\frac{-4s_l\mathrm{Im}f_l}{(\mathrm{Re}f_l-\Delta_l)^2+(\mathrm{Im}f_l-s_l)^2}\ , \tag{16}$$

where

$$\Delta_l=kR_nv_l[G_l(\rho)dG_l(\rho)/d\rho+F_l(\rho)dF_l(\rho)/d\rho]_{r=R_n}\ , \tag{17}$$

$$s_l=kR_nv_l\ , \tag{18}$$

with

$$v_l=1/[F_l^2(\rho)+G_l^2(\rho)]_{r=R_n}\ . \tag{19}$$

The expression (16) for $T_l(E)$ is quite general in the sense that no assumption has so far been made about the interaction for $r<R_n$. The properties of the colliding ions for $r<R_n$ enters into $T_l(E)$ only through the logarthmic derivative f_l.

C. Solution in the region $r<R_n$

In this region, we are to solve the Schrödinger equation with the potential (3a) and choose only that solution which makes the logarithmic derivative complex with the imaginary part being negative. The function $u_l(r)$ (r times the radial wave function) in this region satisfies the equation

$$d^2u_l/d\xi^2+[-\alpha_l+\tfrac{1}{4}\xi^2]u_l=0\ , \tag{20}$$

where

$$\xi=(2\mu\omega/\hbar)^{1/2}(r-R_0)\ , \tag{21}$$

and

$$\alpha_l=-(E-V_l)/(\hbar\omega)\ . \tag{22}$$

The solutions of Eq. (20) are $E(\alpha_l,\xi)$ and $E^*(\alpha_l,\xi)$, where the E's are complex linear functions of the parabolic cylinder functions W (Ref. 14);

$$E(\alpha_l,\xi)=\gamma^{-1/2}W(\alpha_l,\xi)+i\gamma^{1/2}W(a_l,-\xi)\ , \tag{23}$$

$$E^*(\alpha_l,\xi)=\gamma^{-1/2}W(\alpha_l,\xi)-i\gamma^{1/2}W(\alpha_l,-\xi)\ , \tag{24}$$

with

$$\gamma=[1+\exp(2\pi\alpha_l)]^{1/2}-\exp(\pi\alpha_l)\ , \tag{25}$$

and

$$\gamma^{-1}=[1+\exp(2\pi\alpha_l)]^{1/2}+\exp(\pi\alpha_l)\ . \tag{26}$$

The expression for the penetrability function given by Eq. (16) requires that $\mathrm{Im}f_l$ be negative. The required solution, fulfilling this boundary condition and the regularity of the wave function near the origin, is uniquely given by

$$u_l(\xi)=TE^*(\alpha_l,\xi)\ , \tag{27}$$

where T is the amplitude of transmission. The logarithmic derivative, f_l, is then given by

$$f_l=R_n(2\mu\omega/\hbar)^{1/2}\left[\frac{du_l(\xi)/d\xi}{u_l(\xi)}\right]_{r=R_n}\ . \tag{28}$$

Using Eqs. (24), (27), and (28), we obtain, after straightforward algebra, the following expressions for $\mathrm{Re}f_l$ and $\mathrm{Im}f_l$:

$$\mathrm{Re}f_l=R_n(2\mu\omega/\hbar)^{1/2}A/B\ , \tag{29}$$

$$\mathrm{Im}f_l=-R_n(2\mu\omega/\hbar)^{1/2}/B\ , \tag{30}$$

where

$$A=[\gamma^{-1}W(\alpha_l,\xi)dW(\alpha_l,\xi)/d\xi+\gamma W(\alpha_l,-\xi)dW(\alpha_l,-\xi)/d\xi]_{r=R_n}, \tag{31}$$

$$B=[\gamma^{-1}W^2(\alpha_l,\xi)+\gamma W^2(\alpha_l,-\xi)]_{r=R_n}\ . \tag{32}$$

In deriving Eqs. (29) and (30), we have made use of the fact that the Wronskian of the functions $W(\alpha_l,\pm\xi)$ is equal to 1.

The relation of the penetrability function to the logarithmic derivative of the wave function at a

boundary is one of the basic ideas of R-matrix theory. However, the essential difference between the formalism presented here and the R-matrix theory lies in the boundary condition imposed on the logarithmic derivative of the internal wave function. Our treatment of using a complex logarithmic derivative is embedded in the Kapur-Peierls theory[15] as expanded by Brown,[16] whereas Wigner-Eisenbud theory[17] uses a real logarithmic derivative. This treatment, which is basically similar to the theory of Feshbach, Peaslee, and Weisskopf,[13] reduces to the one-level Kapur-Peierls theory provided we impose either purely outgoing or incoming waves as boundary condition on the internal wave function.

D. Asymptotic form of $T_l(E)$

That the penetrability function $T_l(E)$ has the correct asymptotic behavior can be seen as follows. In the high energy limit,

$$\alpha_l \sim -E/\hbar\omega < 0 \ . \tag{33}$$

When α_l is negative, the function $W(\alpha_l,\zeta)$ is oscillatory[14] for all ζ. In such a case, it is convenient to write

$$E^*(\alpha_l,\zeta) = C\exp(-i\chi), \quad (\zeta > 0) \ , \tag{34a}$$

$$dE^*(\alpha_l,\zeta)/d\zeta = -D\exp(-i\phi), \quad (\zeta > 0) \ . \tag{34b}$$

The asymptotic forms of C, D, χ, and ϕ for $|\alpha_l| \gg \zeta^2$ and $\alpha_l < 0$ are

$$C \sim p^{-1/2} \ , \tag{35a}$$

$$D \sim p^{1/2} \ , \tag{35b}$$

$$\chi \sim \pi/4 + p\zeta \ , \tag{35c}$$

$$\phi \sim -\pi/4 + p\zeta \ , \tag{35d}$$

where $p = (-\alpha_l)^{1/2}$. Using Eqs. (35a)–(35d), it is easy to see that the expression for the logarithmic derivative asymptotically reduces to

$$f_l \sim -ikR_n \ , \tag{36}$$

where k is given by Eq. (8).

For the Coulomb functions, it is well known that in the asymptotic limit, i.e., $\rho = kr \gg 1$,

$$\Delta_l \sim 0 \text{ and } s_l \sim kR_n \ . \tag{37}$$

Using Eqs. (36) and (37) into expression (16) for $T_l(E)$, we find that in the high energy limit, $T_l(E) \to 1$.

III. NUMERICAL DETAILS

Instead of using the series expansion, the parabolic cylinder functions $W(\alpha_l,\pm\zeta)$ and their derivatives are evaluated by directly integrating the differential Eq. (20) backward using the method of Runge-Kutta[18] of order four. The starting values for $W(\alpha_l,\zeta)$ and $dW(\alpha_l,\zeta)/d\zeta$ are determined from the asymptotic expansion of the functions for $\zeta^2 - 4\alpha_l \gg 0$, while for $W(\alpha_l,-\zeta)$ and its derivative, closed form expressions for $\zeta = 0$ are used.[14] At the top of the barrier, i.e., for $\alpha_l = 0$, the asymptotic expansion for both $W(\alpha_l,\zeta)$ and its derivative are singular. Hence, near the top of the barrier ($|\alpha_l| < 1$), numerical computation is done using the series expansion. It may be pointed out here that for $|\alpha_l| > 1$, use of series expansion becomes highly inefficient because of the slow convergence rate.

The regular and irregular Coulomb functions are evaluated by using the method of Wills,[19] where, first, the irregular functions $G_l(\rho)$ for $l = 0,1,..,L$ are formed by using the recursion relation. Next, the $G_l(\rho)$ functions are kept recurring to form the sum

$$S = \sum_{i=l}^{\infty} 1/G_i(\rho)G_{i+1}(\rho) \ . \tag{38}$$

The regular functions $F_l(\rho)$ are then obtained from

$$F_L(\rho) = G_L(\rho)S \tag{39}$$

and

$$F_{L-1}(\rho) = G_{L-1}(\rho)S + 1/G_L(\rho) \ . \tag{40}$$

Finally, the backward recursion relation is used to determine $F_l(\rho)$ for $l = L-2, L-3, \ldots, 0$.

IV. RESULTS AND DISCUSSION

Before presenting our results for a number of cases, it would be appropriate to note that (a) we have completely eliminated the discontinuity in the potential which occurs in the treatment of Avishai[10] and Dethier-Stancu,[11] and (b) we have incorporated the effect of the Coulomb potential exactly. We also note that the theory has only three free parameters which are V_0, $\hbar\omega$, and R_n. This is less than those used in many calculations. At high energies, however, it may be necessary to limit the summation over l in Eq. (7) to a critical l_c as is done in the sharp cutoff model[20] calculations. This point will be discussed later.

In the following, we apply this model to calculate the fusion cross sections for the reactions $^{16}O + {}^{16}O$,

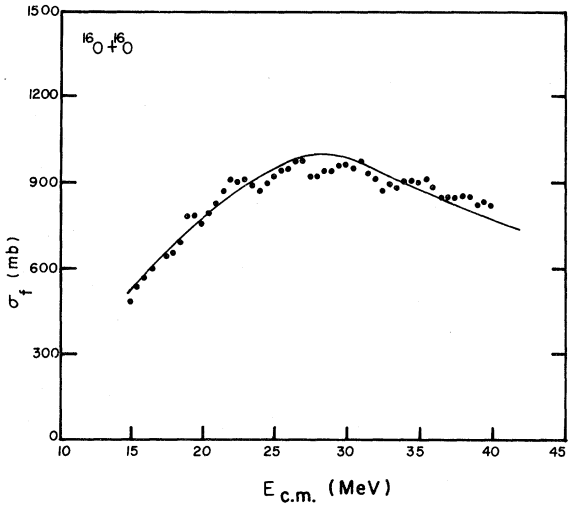

FIG. 1. Comparison of the observed fusion cross section (solid circles) with present calculations (solid line). The experimental data are from Ref. 27.

$^{12}C+^{28,29,30}Si$, $^{16}O+^{24,26}Mg$, $^{16}O+^{28,29,30}Si$, and $^{40}Ca+^{40}Ca$. In Figs. 1–5, we present the experimental data along with our calculated results. In this context, we note that for the $^{40}Ca+^{40}Ca$ reaction, there are two sets of data differing from each other by as much as an order of magnitude. Both the sharp rise in the cross sections in the low energy region and the saturation of the data at higher energies are reproduced quite well by our calculations. For the reactions $^{16}O+^{24,26}Mg$, the calculation slightly overpredicts the data near the shoulder of the excitation function, while for the $^{16}O+^{28,29,30}Si$ reactions, it underpredicts the data in the sub-barrier region. The reason for this underprediction could be attributed to the fact that the model does not take into account the formation of transfer reaction products and the static or dynamic deformations of target and/or projectile which are known to enhance the sub-barrier cross sections.

Regarding the choice of parameters, one approach would have been to search for parameters through a least squared procedure which yields an optimum fit to each data set individually. The stability and trends of the derived parameters would then have served to define the applicability of the model. However, we have done no such search but instead fixed $\hbar\omega$ and allowed only V_0 and R_n to vary. $\hbar\omega$ is fixed at 5.0 MeV for all reactions involving ^{16}O (except for $^{16}O+^{16}O$) and the $^{40}Ca+^{40}Ca$ reaction, and at 8.0 MeV for reactions involving ^{12}C. For the $^{16}O+^{16}O$ reaction, $\hbar\omega$ is taken to be 7.5 MeV. These values of $\hbar\omega$ are chosen so as to get optimum agreement between the calcu-

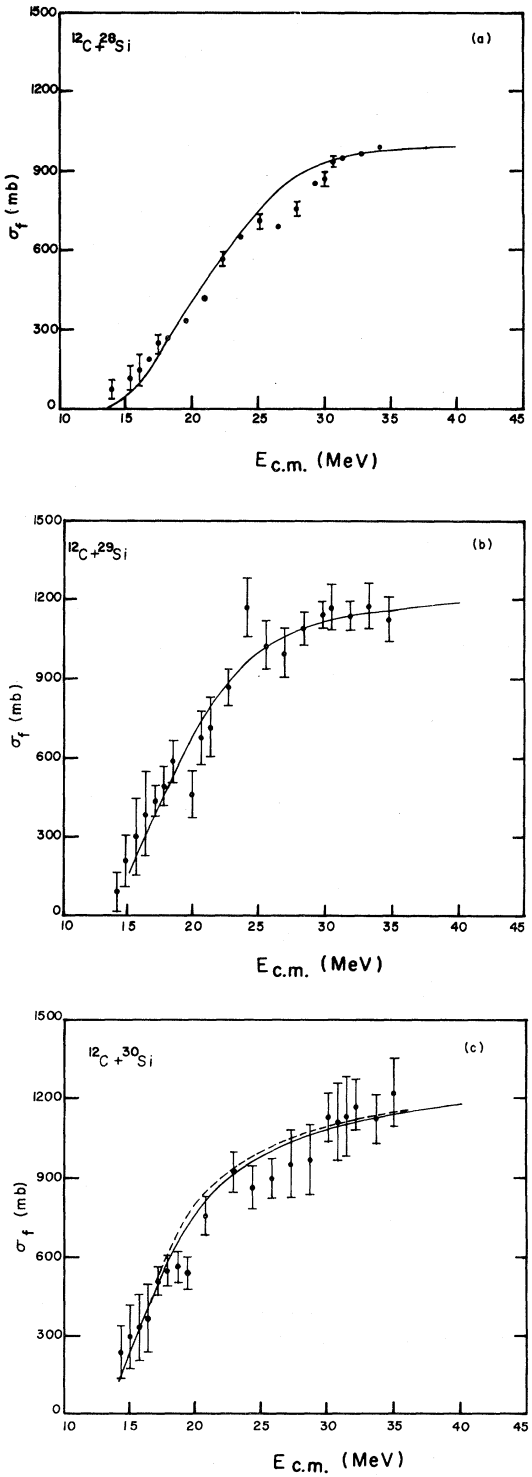

FIG. 2. (a)–(c) The same as that of Fig. 1 except that the data are from Ref. 28. In (c), the dashed line corresponds to calculations with $V_0=17.5$ MeV, $\hbar\omega=7.5$ MeV, and $R_n=7.0$ fm and is shown only where the disagreement with the solid line is large enough to show on the drawing.

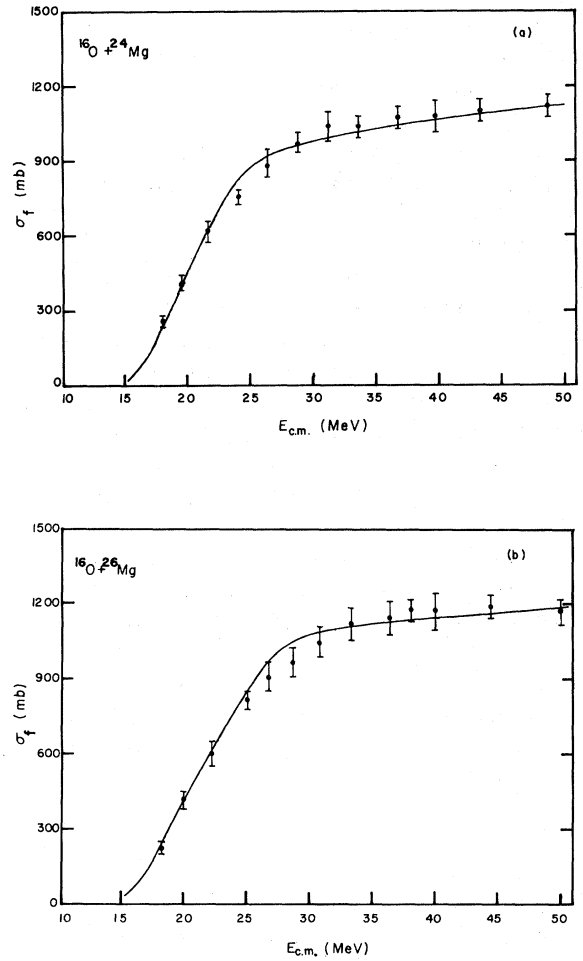

FIG. 3. (a) and (b) The same as that of Fig. 1 except that the data are from Ref. 29.

lated and experimental results. Also, once the value of R_n is fixed for a particular reaction, there is very little room to vary V_0, which is taken to be only slightly greater than $Z_1Z_2e^2/R_n$. This is done in order to avoid the possibility of approximating a substantial portion of the below barrier region by a parabola. Values of the parameters used in the calculations are listed in Table I. Because of the large error bars, other combinations of V_0, $\hbar\omega$, and R_n, which differ slightly from the values in Table I, are also capable of reproducing the data equally well. This is shown in Fig. 2(c) for one of the reactions. The overall effect of the change in the values of the parameters on the magnitude of the fusion cross section is summarized in Table II. The shape of the cross section as a function of energy is, however, mostly controlled by $\hbar\omega$ and V_0, the former being the dominant one.

It is interesting to note in Table I that the parameter r_n, defined by $R_n = r_n(A_1^{1/3} + A_2^{1/3})$, increases

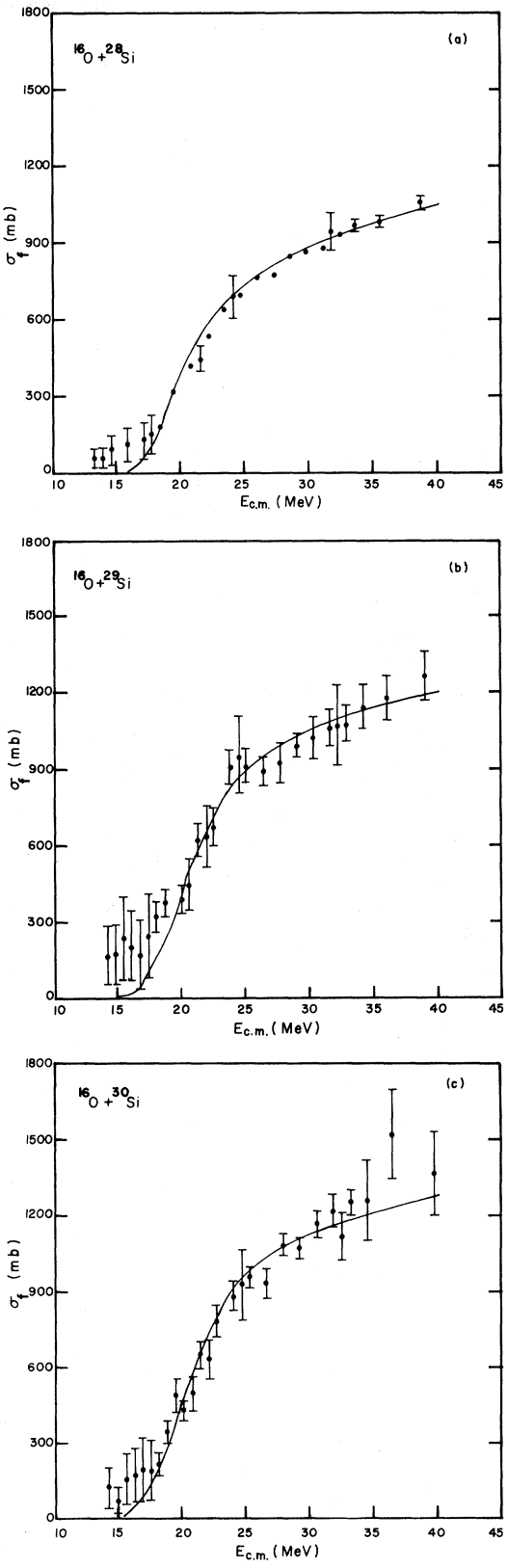

FIG. 4. (a)–(c) The same as that of Fig. 1 except that the data are from Ref. 28.

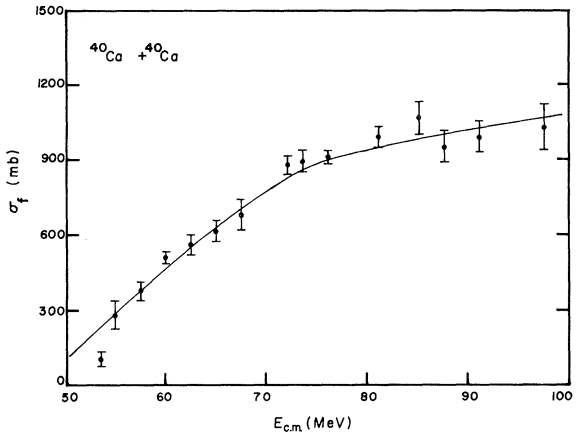

FIG. 5. The same as that of Fig. 1 except that the data are from Ref. 30. As mentioned in the text, it differs from the data of Ref. 31 by almost an order of magnitude.

from ^{28}Si to ^{30}Si for both ^{16}O and ^{12}C projectiles. This is expected because ^{28}Si is the most tightly bound amongst the three, followed by ^{29}Si. It is also well known that ^{24}Mg is more deformed than ^{26}Mg, and hence, one needs a somewhat larger effective radius for the reaction involving ^{24}Mg. It is not surprising to find that both $^{16}O+^{16}O$ and $^{40}Ca+^{40}Ca$ reactions require an r_n greater than that needed for reactions involving Si because, in general, ^{16}O and ^{40}Ca are considered relatively soft and amenable to deformation in the presence of the Coulomb field. In this context, it might be noted that this treatment has tacitly assumed that all nuclei are spherical and the fusion takes place via a static potential.

Some of the existing models[20] demand that the limit to the fusion cross section is set by a critical angular momentum l_c. This is based on a semiclassical picture. For partial waves $l < l_c$, the potential has a "pocket," i.e., a minimum followed by a barrier maximum. As noted by Galin *et al.*,[21] the value V_c of the potential and the radius R_c at this minimum may be the relevant quantities limiting complete fusion during a collision between two complex nuclei. For $l > l_c$, the pocket in the potential disappears (or in the static picture, the effective barrier disappears) and it is no longer possible to form a compound system without breakup, even though the ions may be brought to an arbitrary separation by increasing the bombarding energy. Thus, the critical angular momentum may be viewed as that angular momentum for which the total potential has a local maximum value equal to the incident energy. Semiclassically, corresponding to this critical angular momentum, there is a critical energy E_c beyond which the ions do not fuse for all partial waves, or alternatively, the energy for which the fission barrier vanishes.[22] The critical energy, therefore, corresponds to the maximum in the fusion cross section. Hence, by looking at data, one can deduce l_c from the following approximate semiclassical relation noting that for this l_c the nuclear part of the potential is zero:

$$l_c(l_c+1)=(2\mu R_n^2/\hbar^2)E_c \ . \tag{41}$$

In our calculation, l_c is determined from the experimental maximum of the cross section and is not an additional parameter. Except for the $^{16}O+^{16}O$ reaction, the cross sections of none of the reactions considered here reach maximum and as such we have not used any critical l_c. For the $^{16}O+^{16}O$ reaction, the observed data reaches its maximum at about 28.0 MeV. Thus, using Eq. (41) with $E_c=28.0$ MeV, we obtain $l_c \simeq 26$. As can be seen from Fig. 1 the calculated cross section using this l_c

TABLE I. Values of the best fit parameters $\hbar\omega$, V_0, and R_n, where $R_n=r_n(A_1^{1/3}+A_2^{1/3})$. R_0 is determined by Eq. (6) and $V_c(R_n)=Z_1Z_2e^2/R_n$.

Reaction	Z_1Z_2	$\hbar\omega$ (MeV)	V_0 (MeV)	r_n (fm)	R_n (fm)	R_0 (fm)	$V_C(R_n)$ (MeV)
$^{16}O+^{16}O$	64	7.5	13.0	1.587	8.00	7.48	11.54
$^{12}C+^{28}Si$	84	8.0	21.5	1.155	6.15	5.62	19.70
$^{12}C+^{29}Si$	84	8.0	18.4	1.268	6.80	6.50	17.82
$^{12}C+^{30}Si$	84	8.0	17.5	1.292	6.97	6.84	17.38
$^{16}O+^{24}Mg$	96	5.0	22.7	1.264	6.83	5.91	20.27
$^{16}O+^{26}Mg$	96	5.0	23.8	1.259	6.90	5.78	20.07
$^{16}O+^{28}Si$	112	5.0	23.0	1.314	7.30	6.76	22.13
$^{16}O+^{29}Si$	112	5.0	22.5	1.356	7.58	6.96	21.31
$^{16}O+^{30}Si$	112	5.0	22.0	1.377	7.75	7.14	20.85
$^{40}Ca+^{40}Ca$	400	5.0	56.0	1.601	10.95	10.20	52.69

TABLE II. Summary of the effect of changes in the values of the potential parameters on the fusion cross section. ↑/↓ represents increase/decrease in the values of the parameters and the magnitude of the cross section.

Parameter	Change	Effect on σ_f Low energy	High energy	Comment
$\hbar\omega$	↑	↓	↑	effect is very pronounced
	↓	↑	↓	
V_0	↑	↓	↑	effect is pronounced in the high energy region
	↓	↑	↓	
R_n	↑	↑	↑	increase/decrease in the high energy region are large
	↓	↓	↓	

does follow the data.

If one plots the calculated σ_f as a function of E^{-1}, in all cases the calculated fusion cross section in the low energy region is described by the well known relation[23]

$$\sigma_f = \pi R_f^2 [1 - V(R_f)/E] , \tag{42}$$

where $R_f = r_f(A_1^{1/3} + A_2^{1/3})$ is interpreted as the radius of the interaction barrier $V(R_f)$ which must be overcome in order to reach the critical distance for fusion to occur. A sample case of this behavior is shown in Fig. 6. From this plot, one can determine $V(R_f)$ using the graphical method of Gutbrod *et al.*[24] R_f can then be deduced from the simple relation

$$R_f = Z_1 Z_2 e^2 / V(R_f) . \tag{43}$$

In Table III, we present the values of $V(R_f)$ and R_f deduced from our calculations. For all the reactions, it can be seen that $V(R_f)$ is always a little less than the Coulomb barrier $V_c(R_n)$. This is expected because before the two ions can fuse together, they have to at least overcome the Coulomb barrier. Also, as expected, the interaction barrier height increases considerably with $Z_1 Z_2$.

At this stage it is worth noting that although other calculations such as the one by Glas and Mosel[7] could in many instances reproduce the data, there are some inherent theoretical inadequacies in their formalism which is based on the approximate barrier penetration formula of Hill and Wheeler.[8] As noted by Avishai[10] and Vaz *et al.*,[6] the Hill-Wheeler expression for penertration might be unrealistic in the sub-barrier region in the presence of Coulomb interaction. This is because, in deriving Eq. (1), the asymptotic form of the wave function is taken to be[25]

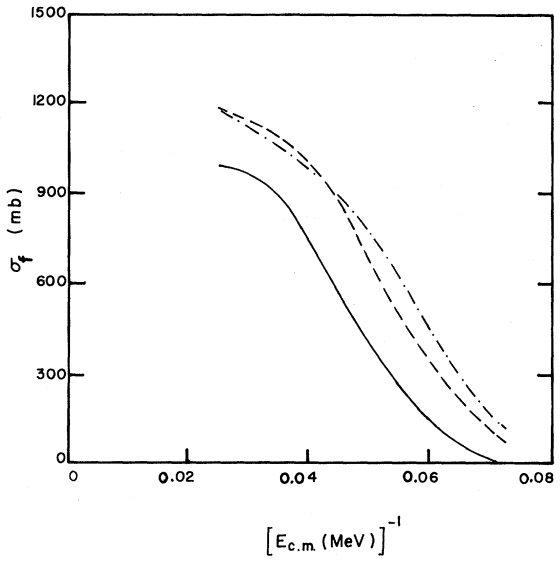

FIG. 6. Plot of the calculated fusion cross sections as a function of $E_{c.m.}^{-1}$ for the reactions $^{12}C+^{28}Si$ (solid line), $^{12}C+^{29}Si$ (dashed line), and $^{12}C+^{30}Si$ (chain line).

TABLE III. A comparison of the values of the interaction barrier height and radius deduced from this calculation with the Glas-Mosel parameters $V(R_B)$ and R_B.

Reaction	Present work $V(R_f)$ (MeV)	r_f (fm)	R_f (fm)	Glas-Mosel $V(R_B)$ (MeV)	R_B (fm)
$^{16}O+^{16}O$	11.10	1.649	8.31	11.0	7.56[a]
$^{12}C+^{28}Si$	16.00	1.421	7.57	15.0	7.40[b]
$^{12}C+^{29}Si$	14.29	1.582	8.48	13.7	8.31[b]
$^{12}C+^{30}Si$	13.33	1.683	9.08	13.7	8.80[b]
$^{16}O+^{24}Mg$	16.67	1.538	8.31	16.0	8.48[c]
$^{16}O+^{26}Mg$	17.09	1.477	8.10	16.6	8.72[c]
$^{16}O+^{28}Si$	17.50	1.661	9.23	16.6	8.06[b]
$^{16}O+^{29}Si$	17.39	1.661	9.29	16.0	8.52[b]
$^{16}O+^{30}Si$	17.09	1.679	9.45	16.4	9.06[b]
$^{40}Ca+^{40}Ca$	50.00	1.687	11.54		

[a]Reference 27.
[b]Reference 28.
[c]Reference 29.

$$\psi=\begin{cases} Te^{i\xi^2/2}\xi^{i\epsilon-1/2}, & r-R_B\gg 0, \quad (44)\\ e^{-i\xi^2/2}|\xi|^{-i\epsilon-1/2}+Re^{i\xi^2/2}|\xi|^{i\epsilon-1/2}, & r-R_B\ll 0, \quad (45)\end{cases}$$

where

$$\xi=(r-R_B)(\mu\omega/\hbar)^{1/2} \quad (46)$$

and

$$\epsilon=(E-V_{Bl})/(\hbar\omega)\ . \quad (47)$$

These asymptotic forms of the wave function are invalid for the Coulomb potential. In fact, asymptotic behaviors (44) and (45) do not properly represent plane waves.

In view of that, we have compared our derived R_f and $V(R_f)$ with the corresponding parameters R_B and $V(R_B)$ of Glas and Mosel and have included them in Table III together with our results. Although they are similar, they could differ by as much as 10%. Of course, Glas and Mosel's calculations use five parameters and we have essentially two (or at best three) parameters.

V. CONCLUSION

In conclusion, it is legitimate to ponder why such a simple parabolic barrier could reproduce the data for fusion. Surely, the nuclear part of the potential is much more complicated. Reasons might simply be that at energies above the Coulomb barrier (or near it), only the top of the nuclear potential comes into play. This part of the ion-ion potential is reasonably approximated in many cases by a smooth parabola as can be seen from the empirical potential used to explain $^{16}O+^{16}O$ or $^{12}C+^{12}C$ elastic scattering data.[3,26] Thus, the energy range of the data analyzed here does not test the real shape of the entire potential but is only sensitive to the structure of the potential near the top. To test the lower part of the nuclear potential, fusion data at energies below the Coulomb barrier are needed.

ACKNOWLEDGMENTS

The authors would like to express their sincere thanks to Dr. John G. Wills of Indiana University for the many discussions and assistance on the numerical methods. One of us (Q.H.) would like to express gratitude to the Office of Research Development and Administration of Southern Illinois University at Carbondale for their financial support.

[1]R. A. Broglia and A. Winther, Phys. Rep. 4C, 155 (1972), and references therein; also see J. P. Bondorf, M. I. Sobel, and D. Sperber, *ibid.* 15C, 85 (1974), and references therein.

[2]G. C. Michaud and E. W. Vogt, Phys. Rev. C 5, 350 (1972); G. C. Michaud, *ibid.* 8, 525 (1973).

[3]Q. Haider and F. B. Malik, *Proceedings of the International Conference on Resonant Behavior of Heavy-Ion Systems, Aegean Sea, —1980,* edited by G. Vourvopoulos (Greek Atomic Energy Commission, Athens, 1981), p. 501.

[4]C. Y. Wong, Phys. Rev. Lett. 31, 766 (1973).

[5]L. C. Vaz and J. M. Alexander, Phys. Rev. C 10, 464 (1974); 18, 2152 (1978).

[6]L. C. Vaz, J. M. Alexander, and G. R. Satchler, Phys. Rep. 69, 375 (1981).

[7]D. E. Glas and U. Mosel, Phys. Rev. C 10, 2620 (1974); Phys. Lett. 49B, 301 (1974); Nucl. Phys. A237, 429 (1975).

[8]D. L. Hill and J. A. Wheeler, Phys. Rev. 89, 1102 (1953); K. W. Ford, D. L. Hill, M. Wakano, and J. A. Wheeler, Ann. Phys. (N.Y.) 7, 239 (1959).

[9]Q. Haider and F. B. Malik, Bull. Am. Phys. Soc. 26, 636 (1981).

[10]Y. Avishai, Z. Phys. A 286, 285 (1978).

[11]J. -L. Dethier and Fl. Stancu, Phys. Rev. C 23, 1503 (1981).

[12]J. M. Blatt and V. F. Weisskopf, *Theoretical Nuclear Physics* (Wiley, New York, 1952), Chap. 8.

[13]H. Feshbach, D. C. Peaslee, and V. F. Weisskopf, Phys. Rev. 71, 145 (1947).

[14]*Handbook of Mathematical Functions,* edited by M. Abramowitz and I. A. Stegun (Dover, New York, 1970), p. 685.

[15]P. L. Kapur and R. Peierls, Proc. R. Soc. London, Ser. A 166, 277 (1938).

[16]G. E. Brown, Rev. Mod. Phys. 31, 893 (1959).

[17]L. Eisenbud and E. P. Wigner, Phys. Rev. 72, 29 (1947); A. M. Lane and R. G. Thomas, Rev. Mod. Phys. 30, 257 (1958).

[18]J. B. Scarborough, *Numerical Mathematical Analysis,* 6th ed. (The John Hopkins Press, Maryland, 1966).

[19]J. G. Wills, J. Comp. Phys. 8, 162 (1971).

[20]M. Lefort, Rep. Prog. Phys. 39, 129 (1976).

[21]J. Galin, D. Guerreau, M. Lefort, X. Tarrago, Phys. Rev. C 9, 1018 (1974).

[22]D. K. Scott, in *Theoretical Methods in Medium-Energy and Heavy-Ion Physics,* edited by K. W. McVoy and W. A. Friedman (Plenum, New York, 1978).

[23]R. Bass, Phys. Rev. Lett. 39, 265 (1977).

[24]H. H. Gutbrod, W. G. Winn, and M. Blann, Nucl. Phys. A213, 267 (1973).

[25]L. D. Landau and E. M. Lifshitz, *Quantum Mechanics* (Pergamon, London, 1975), p. 176.

[26]Q. Haider and F. B. Malik, J. Phys. G 7, 1661 (1981).

[27]J. J. Kolata, R. M. Freeman, F. Haas, B. Heusch, and A. Gallmann, Phys. Rev. C 19, 2237 (1979).

[28]W. J. Jordan, J. V. Maher, and J. C. Peng, Phys. Lett. 87B, 38 (1979).

[29]S. L. Tabor, D. F. Geesaman, W. Henning, D. G. Kovar, and K. E. Rehm, Phys. Rev. C 17, 2136 (1978).

[30]H. Doubre, A. Gamp, J. C. Jacmart, N. Poffe, J. C. Roynette, and J. Wilczynski, Orsay Report No. IPNO-PhN-77-26, 1977; Phys. Lett. 73B, 135 (1978).

[31]E. Tomasi, D. Ardouin, J. Barreto, V. Bernard, H. Doubre, C. Ngo, C. Mazur, E. Piasecki, and R. Ribrag, Fizika (Zagreb) 13, 6 (1981).